Downregulation of hepatic stem cell factor by Vivo-Morpholino treatment inhibits mast cell migration and decreases biliary damage/senescence and liver fibrosis in Mdr2$^{-/-}$ mice

Vik Meadows[1,2,3*], Lindsey Kennedy[2,3*], Laura Hargrove[2], Jennifer Demieville[1], Fanyin Meng[1,3*], Shohaib Virani[2], Evan Reinhart[2], Konstantina Kyritsi[2,3*], Pietro Invernizzi[4#], Zhihong Yang[3], Nan Wu[3], Suthat Liangpunsakul[3], Gianfranco Alpini[1,2,3*] and Heather Francis[1,2,3*]

[1]Research, Central Texas Veterans Health Care System, [2]Department of Medical Physiology, Texas A&M University College of Medicine, Humanitas Clinical and Research Center, Rozzano, Milan, Italy[4]. *present address: [3]Richard L. Roudebush VA Medical Center, and Division of Gastroenterology and Hepatology, Department of Medicine, Indiana University School of Medicine. [#]Present address: Division of Gastroenterology and Center for Autoimmune Liver Diseases, Department of Medicine and Surgery, University of Milano-Bicocca, Monza, Italy.

Address correspondence to:
Heather Francis, Ph.D., FAASLD
Professor of Medicine, VA Research Scientist
Scientific Director, Indiana Center for Liver Research
Richard L. Roudebush VA Medical Center and Indiana University,
Gastroenterology, Medicine
1481 W 10th street
Indianapolis, IN 46202
email: heafranc@iu.edu or heather.francis@va.gov

Conflict of interest: None of the authors have any conflicts to disclose.

This material is the result of work supported by resources at the Central Texas Veterans Health Care System and Richard L. Roudebush VA Medical Center. The views expressed in this article are those of the authors and do not necessarily represent the views of the Department of Veterans Affairs. The studies were supported by a SRCS Award to Dr. Alpini, VA Merit Awards (1I01BX003031, HF; 4I01BX000574, GA; 5I01BX001724, FM) from the United States Department of Veteran's Affairs, Biomedical Laboratory Research and Development Service and NIH NIDDK grant (DK108959, HF) along with funds from Indiana University School of Medicine (GA and HF), Indianapolis, Indiana and Baylor Scott & White Institute (GA and FM), Temple, Texas.

Abstract

Primary sclerosing cholangitis (PSC) is characterized by increased mast cell (MC) infiltration, biliary damage and hepatic fibrosis. Cholangiocytes secrete stem cell factor (SCF), which is a chemoattractant for c-kit expressed on MCs. We aimed to determine if blocking SCF inhibits MC migration, biliary damage and hepatic fibrosis. **Methods:** FVB/NJ and Mdr2$^{-/-}$ mice were treated with Mismatch or SCF Vivo-Morpholinos. We measured (i) SCF expression and secretion; (ii) hepatic damage; (iii) MC migration/activation and histamine signaling; (iv) ductular reaction and biliary senescence; and (v) hepatic fibrosis. In human PSC patients, SCF expression and secretion were measured. *In vitro,* cholangiocytes were evaluated for SCF expression and secretion. Biliary proliferation/senescence was measured in cholangiocytes pretreated with 0.1% BSA or the SCF inhibitor, ISK03. Cultured HSCs were stimulated with cholangiocyte supernatant and activation measured. MC migration was determined with cholangiocytes pretreated with BSA or ISK03 loaded into the bottom of Boyden chambers and MCs into top chamber. **Results**: Biliary SCF expression and SCF serum levels increase in human PSC. Cholangiocytes, but not hepatocytes, from SCF Mismatch Mdr2$^{-/-}$ mice have increased SCF expression and secretion. Inhibition of SCF in Mdr2$^{-/-}$ mice reduced (i) hepatic damage; (ii) MC migration; (iii) histamine and SCF serum levels; and (iv) ductular reaction/biliary senescence/hepatic fibrosis. *In vitro*, cholangiocytes express and secrete SCF. Blocking biliary SCF decreased MC migration, biliary proliferation/senescence, and HSC activation. **Conclusion**: Cholangiocytes secrete increased levels of SCF inducing MC migration, contributing to biliary

damage/hepatic fibrosis. Targeting MC infiltration may be an option to ameliorate PSC progression.

Keywords: mast cells, stem cell factor, fibrosis, PSC, migration

Abbreviations: **ALT** = alanine aminotransferase; **AST** = aspartate aminotransferase; **αSMA** = alpha smooth muscle actin; **CCA** = cholangiocarcinoma; **CK-19** = cytokeratin 19; **c-kit** = KIT proto-oncogene receptor tyrosine kinase; **EIA** = enzyme immunoassay; **FN-1** = fibronectin; **HR** = histamine receptor; **HSC** = hepatic stellate cell; **hHSC** = human hepatic stellate cell; **IBDM** = intrahepatic bile duct mass; **Ki-67** = marker of proliferation; **MC** = mast cell; **Mdr2$^{-/-}$** = multidrug resistance transporter 2/ABC transporter B family member 2 knock out; **mMCP-1** = mouse mast cell protease 1; **p16** = cyclin-dependent kinase inhibitor 2A; **p18** = Cyclin-dependent kinase 4 inhibitor C; **PCNA** = proliferating cell nuclear antigen; **PSC =** primary sclerosing cholangitis; ***q*PCR** = quantitative PCR; **SASP** = senescence-associate secretory phenotype; **SCF =** stem cell factor; **SYP-9** = synaptophysin 9; **WT** = wild type

Introduction

Primary sclerosing cholangitis (PSC) is characterized by increased biliary damage/senescence, inflammation and hepatic fibrosis. Excessive liver fibrosis and collagen deposition causes immense scarring of the liver and eventually, cirrhosis (1, 2). Cholangiocytes are the main liver cell type that is targeted during PSC and upon damage, cholangiocytes secrete a number of neuroendocrine factors (3, 4) and develop a senescence-associated

secretory phenotype (SASP) (5), which is characterized by the secretion of growth factors, interleukins and other mediators including stem cell factor (SCF) (6). Besides ductular reaction, that includes cholangiocyte proliferation and inflammation, senescent cholangiocytes also contribute to hepatic fibrosis by interacting with hepatic stellate cells (HSCs) (7). Currently, PSC is only partly managed by a few approved therapies and/or antibiotic treatments (2). These strategies maintain liver function and decrease the pathological side effects patients suffer from, including pruritis; however, new therapeutic strategies are warranted. For the past decade, researchers have sought to understand the potential signaling mechanisms and pathological indices of PSC using a genetic model, the multi-drug resistant gene 2 ($Mdr2^{-/-}$) mice. This model presents with some of the features that mimic human PSC pathology including biliary damage, inflammation and hepatic fibrosis, damage that can be found as early as 4 weeks of age and worsens as the mice age (8, 9). Previous work has demonstrated that ductular reaction and portal fibrosis are prominent at 12 weeks of age, thus making this time point an excellent tool to study the phenotypes of PSC damage (8-11).

Mast cells (MCs) are immune cells that secrete a number of factors upon degranulation and express various receptors and/or ligands on their surface. MCs are drawn to tissues and/or organs via strong chemoattractants that are expressed or secreted from a variety of cells (12, 13). SCF acts as a primary chemoattractant for MCs by binding to c-Kit (i.e. SCF receptor) on their surface (12, 13). We have demonstrated that, during PSC (both in rodent models and human liver tissues), MC infiltration increases and MCs reside close by bile ducts, allowing for an interaction with cholangiocytes (11, 14). Additionally, it has been shown that cholangiocytes secrete increased amounts of SCF during damage such as cholangiocarcinoma (CCA) and during

liver regeneration (15, 16). Furthermore, there is an increase in c-Kit expression in the livers from Mdr2$^{-/-}$ mice (PSC model) and in human PSC (11, 17). Taken together, these findings suggest that there may be a signaling relationship between cholangiocytes and MCs via SCF/c-Kit.

After migration to the liver, MCs contribute to hepatic fibrosis by promoting HSC activation and also play a role in enhancing inflammation (11, 14, 17). Multiple studies from our group have demonstrated how inhibition of MC mediators (i.e. histamine or histamine receptors) decreases PSC damage and improves cholangiocyte function. Treatment with cromolyn sodium (MC stabilizer) (17, 18) or either the H1 or H2 histamine receptor (HR) antagonists (11) decreases biliary damage, inflammation, and hepatic fibrosis in Mdr2$^{-/-}$ mice. In CCA studies, these compounds blocked tumor growth and angiogenesis and, *in vitro*, we found that inhibition of SCF decreases MC migration, CCA proliferation and angiogenesis (15). These studies set up the rationale for our current study to evaluate the role of the SCF/c-Kit interaction during PSC.

Since our studies have revealed that (i) MC infiltration increases during PSC and (ii) biliary senescence promotes hepatic fibrosis, we aimed to determine if inhibition of biliary SCF decreases MC migration with subsequent decreased biliary damage, inflammation, and hepatic fibrosis.

Methods and Materials

Reagents and other materials

Chemical grade reagents were purchased from Sigma-Aldrich Co (St. Louis, MO) unless stated otherwise. Table 1 contains a list of all antibodies and primers used in the study. Total

RNA was isolated by the TRI Reagent from Sigma Life Science and reverse transcribed with the Reaction Ready First Strand cDNA Synthesis kit (Qiagen, Valencia, CA) (11, 19). For staining in liver sections, samples were sectioned 4-6 μm and 10 fields were analyzed from 3 samples from at least 4 animals per group. For staining in human sections, samples were sectioned at 4-6 μm and 10 fields were analyzed from 3 samples per group.

In vitro, we used a number of cell lines including murine mouse cholangiocytes (immortalized cell line generated in our lab and used by us previously (11, 14)), mouse liver-derived MCs (MC/9, ATCC® CRL-8306™), and human hepatic stellate cells (hHSCs, ScienCell, Carlsbad, CA). All cell lines were maintained according to our published protocols (11). Detailed experiments are described below.

In vivo models

For our animal studies we used the $Mdr2^{-/-}$ mouse model of PSC, which are raised on FVB/NJ background (wild-type, WT) (8, 17). Male WT and $Mdr2^{-/-}$ mice were treated with either Mismatch Morpholino (CTTGTTGATAACGAAAGCCACCGCT) or SCF Vivo-Morpholino (CTTCTTCATAAGGAAAGGCAGCGCT) given by tail vein injection 2x/week for 1 week (4 μg/100 μl NaCl) as described (20, 21). Male mice (4 mice per group) were euthanized at 12 weeks of age, which display an increase in PSC-induced hepatic damage (10, 17). All mice were kept in standard conditions including 12/12 light dark cycle and standard chow and water. From these groups of mice, we collected liver blocks (frozen and paraffin-embedded), serum, isolated cholangiocytes and hepatocytes, as described (17, 19). Cholangiocyte (1 million cells/100 μl) and hepatocyte (1 million cells/100 μl) supernatants were collected after incubation at 37° for 4-6 hours.

SCF Expression and Secretion

In WT and Mdr2$^{-/-}$ mice treated with either Mismatch or Vivo-Morpholino, we measured SCF expression (co-stained with either CK-18 to mark hepatocytes or CK-19 to identify SCF-positive cholangiocytes) by immunofluorescence as previously described by us using frozen liver sections (4-6 um) (17). SCF secretion was measured in serum and isolated cholangiocyte or hepatocyte supernatants by EIA (16). By western blotting, we measured SCF expression in both total liver and isolated hepatocytes, as well as hepatocyte gene expression by *q*PCR.

To determine SCF expression patients with PSC, human liver sections from normal controls (collected as part of liver CCA resection and considered non-diseased areas) and PSC patients were used (Table 2). PSC patients presented with late PSC phenotypes, as described in our previous work (17). Liver sections were obtained by needle biopsies from three control patients and three late stage PSC (with or without cirrhosis) along with the collection of serum. The de-identified samples were provided by Dr. Pietro Invernizzi under a protocol approved by Humanitas Research Hospital; the protocol was approved by the Central Texas Veteran's Health Care System Institutional Review Board and Research Development Committee. SCF/CK-19 immunofluorescence (with 3D zoom) was performed to identify SCF-positive cholangiocytes in human control and PSC samples and EIA was used to determine SCF serum secretion.

Hepatic Damage

Hepatic damage including necrosis and inflammation was determined in paraffin-embedded liver sections (4-5 μm thick) by Hematoxylin & Eosin Y (H&E) staining in all groups of mice. Aspartate aminotransferase (AST) and alanine transaminase (ALT) were determined by IDEXX Catalyst One test slides (IDEXX, Westbrook, ME) in serum from all groups of mice (5, 7).

Mast Cell Infiltration/Activation and Histamine Signaling

The presence of MCs was detected by immunohistochemistry for mouse MC protease-1 (mMCP-1) in paraffin-embedded liver sections (4-5 μm thick) from WT and Mdr2$^{-/-}$ mice treated with Mismatch or SCF Vivo-Morpholino (11, 19). Histamine secretion was measured by EIA (11, 17) in serum from all groups of mice and the mRNA expression of histamine receptors (HRs) 1-4 and MC markers: chymase, tryptase, and c-kit (17) were determined in total liver by *q*PCR.

Intrahepatic Bile Duct Mass (IBDM), Biliary Proliferation, Hepatic Fibrosis, and Cholangiocyte Senescence

In all groups of mice, we measured the following: IBDM was determined by immunohistochemistry in paraffin-embedded liver sections (4-6 μm) for CK-19, whereas biliary proliferation was measured by Ki-67 immunohistochemistry in paraffin-embedded liver sections. Both IBDM and biliary proliferation were semi-quantified using a light microscope and Image-Pro Analyzer, DC Imaging, West Chester, OH (5, 11, 20).

To determine the effects of SCF inhibition on hepatic fibrosis, we performed Sirius Red/Fast Green staining in liver sections (with semi-quantification) and *q*PCR for α-smooth muscle actin (α-SMA) in total liver (11, 14, 17). HSC presence was determined by immunofluorescence for desmin in all groups of mice in frozen liver sections.

Since SCF is also considered to be a cellular senescence-associated secretory phenotype (SASP) (6), we determined if biliary senescence was changed in cholangiocytes. Mice were evaluated for senescent factors including p18 by *q*PCR and p16 by immunofluorescence in frozen liver sections (4-6 μm thick) co-stained with CK-19 to image bile ducts (7, 21).

***In Vitro* Studies**

First, immortalized murine cholangiocyte lines (11, 22) were evaluated for SCF expression and cultured MCs (14, 17) evaluated for c-Kit expression by immunofluorescence. To validate our *in vivo* findings, we next determined the effects of SCF inhibition on biliary proliferation by treating cultured cholangiocytes with the SCF inhibitor, ISCK03 (10 μM, 24 hrs (abcam, Cambridge, MA) dissolved in 0.1% DMSO (15)) before evaluating PCNA mRNA expression by *q*PCR. In addition, biliary senescence was measured in cholangiocytes treated with control or the SCF inhibitor by measuring the expression of p16 and p18 by *q*PCR.

Using cultured human HSCs (hHSCs) (11), we determined if there was a direct effect on HSC activation via biliary SCF. Supernatants from immortalized murine cholangiocyte lines were collected by centrifugation after treatment with the SCF inhibitor (or vehicle control) and cocultured with hHSCs for 48 hrs, before measuring Synaptophysin-9 (SYP-9) and fibronectin (FN-1) by *q*PCR (11, 17).

Finally, since cholangiocytes secrete SCF and we hypothesize that increased SCF induces MC migration, we performed *in vitro* studies to block this interaction. Murine cholangiocyte lines were placed in the bottom of a Boyden Chamber and subsequently treated with the SCF inhibitor, ISCK03 (10 μM) for 24 hrs to inhibit biliary SCF/c-kit signaling (15). After 24 hrs, MCs were then placed in the upper chamber and migration through the membrane (Corning® BioCoat™ Matrigel® Invasion Chamber with PET 8 μm membrane) was evaluated after 24 hrs. Following methanol fixation, MC presence in the transwell membrane was determined by Toluidine Blue staining and semi-quantified using a light microscope (15).

Statistical Analysis

All data is expressed as mean ± SEM. Groups were analyzed by the Student unpaired t test when two groups are analyzed or a two-way ANOVA when more than two groups are analyzed, followed by an appropriate post hoc test. $p<0.05$ was considered significant.

Results

SCF biliary expression and secretion increases in human PSC and Mdr2$^{-/-}$ mice treated with Mismatch Morpholino

By immunofluorescence, we demonstrated that SCF expression (primarily in cholangiocytes identified by CK-19 staining) increased in patients with late-stage PSC compared to control tissues collected from non-diseased areas (Figure 1A). Further, patients with PSC have an increased amount of circulating SCF compared to controls (Figure 1B). In WT mouse groups, there were no changes in SCF expression (Supplemental Figure 1); however, Mdr2$^{-/-}$ mice treated with mismatch Morpholino have increased SCF expression (primarily in cholangiocytes) shown by immunofluorescence (Figure 1C), which was absent in mice treated with SCF Vivo-Morpholino (Figure 1C). In serum from WT Mismatch and SCF Vivo-Morpholino, SCF levels were unchanged; however, Mdr2$^{-/-}$ Mismatch mice had increased amounts of SCF that was reduced in Mdr2$^{-/-}$ SCF Vivo-Morpholino mice (Figure 1D). Finally, biliary secretion of SCF was increased in Mdr2$^{-/-}$ mice treated with Mismatch compared to WT (no changes were noted between WT groups) which was decreased in cholangiocyte supernatants from Mdr2$^{-/-}$ mice treated with SCF Vivo-Morpholino (Figure 1E).

Hepatocyte SCF expression and secretion are unchanged in Mdr2$^{-/-}$ mice treated with Mismatch or SCF Vivo-Morpholino

We found that SCF expression did not markedly change in total liver or isolated hepatocytes between all groups as shown by western blotting (Supplemental Figure 2A) and immunofluorescence (WT groups not shown), Supplemental Figure 2B). In addition, hepatocyte SCF mRNA and protein expression did not significantly increase in Mdr2$^{-/-}$ SCF Mismatch mice when compared to WT SCF Mismatch (Supplemental Figure 2A-C). Finally, hepatocyte SCF secretion was not increased in Mdr2$^{-/-}$ SCF Mismatch mice compared to WT SCF Mismatch; there was no difference between Mdr2$^{-/-}$ treated with SCF Mismatch or Vivo-Morpholino (Supplemental Figure 2D). This data supports our theory that biliary SCF (but not hepatocyte SCF) is critical to MC migration and subsequent damage during PSC progression.

Hepatic damage decreases in Mdr2$^{-/-}$ mice treated with SCF Vivo-Morpholino

By H&E, we found that inhibition of SCF decreased hepatic necrosis and portal inflammation in Mdr2$^{-/-}$ mice treated with Mismatch (Supplemental Figure 3A); there were no changes between WT Mismatch and SCF Vivo-Morpholino treatments. H&E in human PSC shows ductular reaction, necrosis and inflammation when compared to human controls (Supplemental Figure 3B) The levels of AST and ALT increased in Mdr2$^{-/-}$ mice treated with Mismatch compared to WT mice, which were reduced when Mdr2$^{-/-}$ mice were treated with SCF Vivo-Morpholino (Supplemental Figure 3C).

Inhibition of SCF decreased MC migration/activation and histamine signaling

Serum histamine levels were decreased in WT mice treated with SCF Vivo-Morpholino compared to Mismatch and, in Mdr2$^{-/-}$ mice treated with Mismatch, histamine levels were significantly increased compared to both WT groups, which was reduced in Mdr2$^{-/-}$ mice treated with SCF Vivo-Morpholino (Figure 2A). By immunohistochemistry for mMCP-1 there were no

MCs found in WT mice treated with Mismatch or SCF Vivo-Morpholino, which is consistent with our previous work showing that WT mice typically display few to no MCs around the portal area (11). In Mismatch Mdr2$^{-/-}$ mice, MC presence was increased in the portal area (inset: red arrows = MCs; black arrow = bile duct); which was reduced in Mdr2$^{-/-}$ mice treated with SCF Vivo-Morpholinos (Figure 2B). Further, the mRNA expression of MC markers increased in Mdr2$^{-/-}$ Mismatch mice compared to WT (no difference between Mismatch and SCF Vivo-Morpholino treatment) and were reduced in SCF Vivo-Morpholino Mdr2$^{-/-}$ mice (Supplemental Figure 4A). Finally, the expression levels of H1-H4 HRs were increased in Mdr2$^{-/-}$ mice treated with Mismatch compared to WT (no difference between Mismatch and SCF Vivo-Morpholino); however, blocking SCF in Mdr2$^{-/-}$ mice resulted in the reduction of H1, H2 and H4 HR, whereas H3 HR was not changed (Supplemental Figure 4B).

IBDM, biliary proliferation, hepatic fibrosis, and senescence decreased after inhibition of SCF in Mdr2$^{-/-}$ mice

In WT Mismatch and SCF Vivo-Morpholino treated mice there was no difference in IBDM, biliary proliferation, hepatic fibrosis, and cholangiocyte senescence (Figures 3, 4, 5). Mdr2$^{-/-}$ mice treated with Mismatch displayed an increase in (i) IBDM and biliary proliferation as shown by CK-19 and Ki-67, respectively (Figure 3A and 3B); (ii) collagen deposition, primarily around the portal area (Figure 4A) and supported by semi-quantification (Figure 4B); (iii) HSC presence shown by immunofluorescence for desmin (Figure 4C) along with the mRNA expression of α-SMA (Figure 4D); and (iv) biliary p18 and p16 expression (Figure 5A-5B). All of these parameters decreased in Mdr2$^{-/-}$ mice treated with SCF Vivo-Morpholino demonstrating that manipulation of SCF regulates liver damage (Figures 3-5).

Inhibition of biliary SCF decreased (i) cholangiocyte proliferation/senescence, (ii) hHSC activation; and (iii) MC migration, *in vitro*

In vitro, by immunofluorescence, we found that (i) cholangiocytes express SCF and (ii) MCs express c-Kit (Figure 6A). By *q*PCR, the expression of PCNA (Figure 6B) and the senescent markers, p16 and p18 (Figure 6C) all decreased after cholangiocytes were treated with the SCF inhibitor (ISCK03). These results support our *in vivo* studies that demonstrate that inhibition of SCF decreases biliary damage and senescence. Similarly, we measured HSC activation *in vitro* after stimulation with cholangiocyte supernatants (control and pre-treatment with the SCF inhibitor) and found that inhibition of biliary SCF decreases hHSC activation by reducing the expression of SYP-9 and FN-1 shown by *q*PCR (Supplemental Figure 5). *In vitro*, blocking cholangiocyte SCF signaling decreased (i) secretion of biliary SCF (Figure 7A) and (ii) MC migration toward cholangiocytes assayed by Boyden Chamber migration (Figure 7B) and quantified using Toluidine Blue staining (Figure 7C).

Discussion

Our current study demonstrates that increased biliary SCF may induce MC migration to the liver following damage. We show that patients with PSC have increased biliary SCF expression and serum levels that are also reflected in $Mdr2^{-/-}$ mice treated with Mismatch Morpholinos. Biliary, but not hepatocyte, SCF secretion increases in $Mdr2^{-/-}$ Mismatch mice suggesting that our findings are cholangiocyte-specific. Inhibition of SCF using Vivo-Morpholino treatment decreased (i) biliary damage/senescence, (ii) MC migration and histamine signaling and (iii) hepatic fibrosis. Our *in vitro* studies demonstrated that inhibition of biliary SCF inhibited

MC migration. Taken together our study highlights the potential therapeutic effects of blocking MC migration and activation via inhibition of SCF.

SCF has been touted as one of the most critical regulators of MC migration, degranulation and activation as well as being responsible for MC phenotype after migration, and the SCF/c-Kit interaction has been studied extensively in tumorigenesis, wound healing and allergic responses (23). The SCF/c-Kit interaction has been shown to contribute to the development and progression of intrahepatic CCA (24). It has been shown that CCA tumors have 20-fold higher expression of SCF than normal tissue, which supports our findings that SCF expression and secretion increase in human PSC. Since PSC patients are at greater risk for CCA (1) and SCF is enhanced in both PSC and CCA (15), it might be feasible that SCF is a regulator of the transition between PSC and CCA. Aside from being a growth factor, SCF is a well-known chemoattractant, and studies using a mutant MC line that lacks c-Kit demonstrate that MC migration is inhibited, but migration was not altered by interleukin (IL)-3 stimulation (25) suggesting that the SCF/c-Kit relationship may be tightly regulated.

Besides SCF/c-Kit, there are studies demonstrating various chemoattractants which induce MC migration and activation. In rat peritoneal MCs, tumor necrosis factor (TNF, a potent MC chemoattractant (12)) induced MC migration, that was blocked when either TNF or TNF-receptor 1 antibodies were used (26), and the interleukin (IL)-33 has also been described as a potent chemoattractant as well as inducing MC degranulation. The classic FCεR1/IgE interaction is a regulator of MC migration and degranulation especially during allergic responses and asthmatic episodes (27). Similar to our findings demonstrating decreased hepatic damage after blocking SCF, inhibition of SCF/c-Kit also reduced pulmonary hypertension and vascular

remodeling in a model of chronic hypoxia (28). Further, in a model of pancreatic cancer, inhibition of SCF/c-Kit blocked invasion and metastasis via PI3K/AKT and ERK signaling (29).

PSC is characterized by hepatic fibrosis and our current study supports our previous work demonstrating that blocking MC infiltration and degranulation decreases liver fibrosis and HSC activation (11, 14, 15, 17, 18). To support this, it has been shown that the SCF/c-Kit interaction promotes renal interstitial fibrosis (30). Similar to our current findings, the authors found that, in a diabetic kidney disease model, the expression of fibronectin and collagen type-1a increases in diseased rats compared to normal and this was associated with increased SCF and c-Kit gene expression (30). Additionally, following 70% partial hepatectomy, SCF levels increase over time and peak at 7 days (16). This study demonstrated that SCF contributes to biliary remodeling and liver regeneration via increased chemokine and cytokine signaling, which supports our current study that SCF may alter biliary senescence and contribute to damage and hepatic fibrosis.

Biliary senescence is a feature that has been found to regulate PSC and may contribute to an increase in damage and hepatic fibrosis (5, 7). When cholangiocytes become senescent they develop a SASP that is characterized by an increase in the release of inflammatory mediators including TGF-β1 and SCF. Since MCs are found in close proximity to bile ducts, we hypothesize that senescent cholangiocytes may drive MC infiltration following liver injury. In support of this, most of the chemoattractants that promote MC migration are considered SASP factors that are secreted by cholangiocytes upon damage and include: SCF; growth factors like vascular endothelial growth factor and nerve growth factor; and interleukins such as IL-6 and IL-8 (6). Our work herein demonstrates that inhibition of SCF/c-Kit signaling decreases biliary

senescence with a subsequent decrease in MC activation and hepatic damage. Interestingly, we did not find any alterations in TGF-β1 expression after inhibition of SCF (data not shown). The neuroendocrine phenotype that is displayed in cholangiocytes during ductular reaction (4) potentially supports MC migration and subsequent degranulation, which contributes to enhanced disease progression.

Targeted therapies for PSC are significantly lacking, and the current study and previous work from our lab present the novel concept of potential targeted therapy via manipulation of MCs and their mediators. In MC-deficient mice subjected to bile duct ligation, we found a decrease in biliary damage, inflammation and hepatic fibrosis, but when MC-deficient mice (typically normal livers void of damage) were subjected to tail vein injections of cultured MCs, biliary injury and collagen deposition significantly increased (14). While more studies are warranted to understand MC migration *in vivo;* our study presents the novel concept that blocking biliary senescence/SASP decreases MC presence and subsequent liver damage. This study also demonstrates the critical role that MCs play during liver injury and their significant contribution to disease progression. Since MCs are not critical to the overall function of the liver, targeting their mediators or activation may be an alternative strategy to battling PSC and other liver diseases.

References:

1. Lee CW, Ronnekleiv-Kelly S. Autoimmune Diseases of the Biliary Tract: A Review. Surg Clin North Am 2019;99:185-201.

2. Rajapaksha IG, Angus PW, Herath CB. Current therapies and novel approaches for biliary diseases. World J Gastrointest Pathophysiol 2019;10:1-10.

3. Alvaro D, Mancino MG, Glaser S, Gaudio E, Marzioni M, Francis H, Alpini G. Proliferating cholangiocytes: a neuroendocrine compartment in the diseased liver. Gastroenterology 2007;132:415-431.

4. Sato K, Marzioni M, Meng F, Francis H, Glaser S, Alpini G. Ductular Reaction in Liver Diseases: Pathological Mechanisms and Translational Significances. Hepatology 2019;69:420-430.

5. Wu N, Meng F, Zhou T, Venter J, Giang TK, Kyritsi K, Wu C, et al. The Secretin/Secretin Receptor Axis Modulates Ductular Reaction and Liver Fibrosis through Changes in Transforming Growth Factor-beta1-Mediated Biliary Senescence. Am J Pathol 2018;188:2264-2280.

6. Coppe JP, Desprez PY, Krtolica A, Campisi J. The senescence-associated secretory phenotype: the dark side of tumor suppression. Annu Rev Pathol 2010;5:99-118.

7. Zhou T, Wu N, Meng F, Venter J, Giang TK, Francis H, Kyritsi K, et al. Knockout of secretin receptor reduces biliary damage and liver fibrosis in Mdr2(-/-) mice by diminishing senescence of cholangiocytes. Lab Invest 2018;98:1449-1464.

8. Popov Y, Patsenker E, Fickert P, Trauner M, Schuppan D. Mdr2 (Abcb4)-/- mice spontaneously develop severe biliary fibrosis via massive dysregulation of pro- and antifibrogenic genes. J Hepatol 2005;43:1045-1054.

9. Trauner M, Fickert P, Baghdasaryan A, Claudel T, Halilbasic E, Moustafa T, Wagner M, et al. New insights into autoimmune cholangitis through animal models. Dig Dis 2010;28:99-104.

10. Fickert P, Wagner M, Marschall HU, Fuchsbichler A, Zollner G, Tsybrovskyy O, Zatloukal K, et al. 24-norUrsodeoxycholic acid is superior to ursodeoxycholic acid in the treatment of sclerosing cholangitis in Mdr2 (Abcb4) knockout mice. Gastroenterology 2006;130:465-481.

11. Kennedy L, Hargrove L, Demieville J, Karstens W, Jones H, DeMorrow S, Meng F, et al. Blocking H1/H2 histamine receptors inhibits damage/fibrosis in Mdr2(-/-) mice and human cholangiocarcinoma tumorigenesis. Hepatology 2018.

12. Halova I, Draberova L, Draber P. Mast cell chemotaxis - chemoattractants and signaling pathways. Front Immunol 2012;3:119.

13. Sibilano R, Frossi B, Pucillo CE. Mast cell activation: a complex interplay of positive and negative signaling pathways. Eur J Immunol 2014;44:2558-2566.

14. Hargrove L, Kennedy L, Demieville J, Jones H, Meng F, DeMorrow S, Karstens W, et al. Bile duct ligation-induced biliary hyperplasia, hepatic injury, and fibrosis are reduced in mast cell-deficient Kit(W-sh) mice. Hepatology 2017;65:1991-2004.

15. Johnson C, Huynh V, Hargrove L, Kennedy L, Graf-Eaton A, Owens J, Trzeciakowski JP, et al. Inhibition of Mast Cell-Derived Histamine Decreases Human Cholangiocarcinoma Growth and Differentiation via c-Kit/Stem Cell Factor-Dependent Signaling. Am J Pathol 2016;186:123-133.

16. Meng F, Francis H, Glaser S, Han Y, DeMorrow S, Stokes A, Staloch D, et al. Role of stem cell factor and granulocyte colony-stimulating factor in remodeling during liver regeneration. Hepatology 2012;55:209-221.

17. Jones H, Hargrove L, Kennedy L, Meng F, Graf-Eaton A, Owens J, Alpini G, et al. Inhibition of mast cell-secreted histamine decreases biliary proliferation and fibrosis in primary sclerosing cholangitis Mdr2-/- mice. Hepatology 2016.

18. Kennedy LL, Hargrove LA, Graf AB, Francis TC, Hodges KM, Nguyen QP, Ueno Y, et al. Inhibition of mast cell-derived histamine secretion by cromolyn sodium treatment decreases biliary hyperplasia in cholestatic rodents. Lab Invest 2014;94:1406-1418.

19. Kennedy L, Hargrove L, Demieville J, Bailey J, Dar W, Polireddy K, Chen Q, et al. Knockout of l-Histidine Decarboxylase Prevents Cholangiocyte Damage and Hepatic Fibrosis in Mice Subjected to High-Fat Diet Feeding via Disrupted Histamine/Leptin Signaling. Am J Pathol 2017.

20. Kyritsi K, Meng F, Zhou T, Wu N, Venter J, Francis H, Kennedy L, et al. Knockdown of Hepatic Gonadotropin-Releasing Hormone by Vivo-Morpholino Decreases Liver Fibrosis in Multidrug Resistance Gene 2 Knockout Mice by Down-Regulation of miR-200b. Am J Pathol 2017;187:1551-1565.

21. Wan Y, McDaniel K, Wu N, Ramos-Lorenzo S, Glaser T, Venter J, Francis H, et al. Regulation of Cellular Senescence by miR-34a in Alcoholic Liver Injury. Am J Pathol 2017;187:2788-2798.

22. Ueno Y, Alpini G, Yahagi K, Kanno N, Moritoki Y, Fukushima K, Glaser S, et al. Evaluation of differential gene expression by microarray analysis in small and large cholangiocytes isolated from normal mice. Liver Int 2003;23:449-459.

23. Galli SJ, Tsai M, Wershil BK. The c-kit receptor, stem cell factor, and mast cells. What each is teaching us about the others. Am J Pathol 1993;142:965-974.

24. Mansuroglu T, Ramadori P, Dudas J, Malik I, Hammerich K, Fuzesi L, Ramadori G. Expression of stem cell factor and its receptor c-Kit during the development of intrahepatic cholangiocarcinoma. Lab Invest 2009;89:562-574.

25. Meininger CJ, Yano H, Rottapel R, Bernstein A, Zsebo KM, Zetter BR. The c-kit receptor ligand functions as a mast cell chemoattractant. Blood 1992;79:958-963.

26. Brzezinska-Blaszczyk E, Pietrzak A, Misiak-Tloczek AH. Tumor necrosis factor (TNF) is a potent rat mast cell chemoattractant. J Interferon Cytokine Res 2007;27:911-919.

27. Abramson J, Pecht I. Regulation of the mast cell response to the type 1 Fc epsilon receptor. Immunol Rev 2007;217:231-254.

28. Young KC, Torres E, Hehre D, Wu S, Suguihara C, Hare JM. Antagonism of stem cell factor/c-kit signaling attenuates neonatal chronic hypoxia-induced pulmonary vascular remodeling. Pediatr Res 2016;79:637-646.

29. Zhang M, Ma Q, Hu H, Zhang D, Li J, Ma G, Bhat K, et al. Stem cell factor/c-kit signaling enhances invasion of pancreatic cancer cells via HIF-1alpha under normoxic condition. Cancer Lett 2011;303:108-117.

30. Yin DD, Luo JH, Zhao ZY, Liao YJ, Li Y. Tranilast prevents renal interstitial fibrosis by blocking mast cell infiltration in a rat model of diabetic kidney disease. Mol Med Rep 2018;17:7356-7364.

Figure legends

Figure 1: SCF expression and secretion in PSC patients and in Mdr2$^{-/-}$ mice. SCF expression shown by immunofluorescence (CK-19 (green) and SCF (red)) (A) and serum secretion (B) increase in patients with PSC compared to controls. In Mdr2$^{-/-}$ mice treated with Mismatch there is increased SCF expression (co-localized with CK-19 (red) to mark SCF-positive bile ducts) (C) and serum secretion (D) that are reduced when mice are treated with the SCF Vivo-Morpholino (C-D). There were no changes in SCF serum secretion between WT Mismatch and WT SCF Vivo-Morpholino (D). Cholangiocyte SCF secretion increased in supernatants from Mdr2$^{-/-}$ Mismatch mice compared to WT groups; however, SCF secretion was blocked in cholangiocyte supernatants from Mdr2$^{-/-}$ mice treated with SCF Vivo-Morpholino (E). Data are mean ± SEM of 9-12 experiments for *q*PCR and 15 experiments for EIA. *p<0.05 vs. WT SCF Mismatch; #p<0.05 vs. Mdr2$^{-/-}$ SCF Mismatch mice. Representative images x80.

Figure 2: MC migration/activation and histamine signaling in WT and Mdr2$^{-/-}$ mice treated with SCF Mismatch or SCF Vivo-Morpholinos. Serum histamine levels were decreased in WT mice treated with SCF Vivo-Morpholino compared to Mismatch. In Mdr2$^{-/-}$ Mismatch mice, serum histamine increased, but was reduced back to WT levels in Mdr2$^{-/-}$ mice treated with SCF Vivo-Morpholino (A). By immunohistochemistry for m-MCP1 no MCs were detected in either WT group; however, there was an infiltration of MCs in Mdr2$^{-/-}$ mice treated with Mismatch (red arrows (MCs) and black arrow (bile duct) shown in insert). Mdr2$^{-/-}$ mice treated with SCF Vivo-Morpholino did not display any MC migration/infiltration (B). Data are mean ± SEM of 12 experiments for EIA. *p<0.05 vs. WT SCF Mismatch; #p<0.05 vs. Mdr2$^{-/-}$ SCF Mismatch mice. Representative images x20 (inset images = 100x).

Figure 3: IBDM and biliary proliferation in WT and Mdr2$^{-/-}$ mice treated with SCF Mismatch or SCF Vivo-Morpholinos. By immunohistochemistry and semi-quantification for CK-19 (A) and Ki-67 (B) we found that IBDM and biliary proliferation were unchanged in WT groups; however, there was a significant increase in Mdr2$^{-/-}$ Mismatch treated mice. Further, inhibition of SCF in Mdr2$^{-/-}$ mice reduced both IBDM (A) and biliary proliferation (B) compared to Mdr2$^{-/-}$ Mismatch mice. Data are mean ± SEM of 10 experiments from 4 mice per group. *p<0.05 vs. WT SCF Mismatch; #p<0.05 vs. Mdr2$^{-/-}$ SCF Mismatch mice. Representative images x20.

Figure 4: Hepatic fibrosis and HSC activation in WT and Mdr2$^{-/-}$ mice treated with SCF Mismatch or SCF Vivo-Morpholinos. Collagen deposition shown by Sirius Red/Fast Green staining (A) and semi-quantification (B) was unchanged in WT groups, but significantly increased in Mdr2$^{-/-}$ mice treated with Mismatch. When Mdr2$^{-/-}$ mice were treated with SCF Vivo-Morpholino, collagen deposition was reduced compared to Mdr2$^{-/-}$ Mismatch mice (A-B). The expression of desmin (C) and the gene expression of α-SMA (D) did not change in WT groups; however, there was a significant increase in both found in Mdr2$^{-/-}$ Mismatch mice that was reduced in the Mdr2$^{-/-}$ mice treated with SCF Vivo-Morpholino (C-D). Data are mean ± SEM of 10 experiments from 4 mice per group for Sirius Red/Fast Green staining and 12 experiments for *q*PCR. *p<0.05 vs. WT SCF Mismatch; #p<0.05 vs. Mdr2$^{-/-}$ SCF Mismatch mice. Representative images x40.

Figure 5: Biliary senescence in WT and Mdr2$^{-/-}$ mice treated with SCF Mismatch or SCF Vivo-Morpholinos. By real-time PCR (A) we found no change between WT groups in the expression of p18; however, there was an increase in p18 expression in Mdr2$^{-/-}$ Mismatch mice which was reduced when Mdr2$^{-/-}$ mice were treated with SCF Vivo-Morpholinos (A). By immunofluorescence (B) we found an increased expression of p16 in cholangiocytes (marked by white arrows to show co-localization) in Mdr2$^{-/-}$ Mismatch mice compared to controls that was decreased in Mdr2$^{-/-}$ mice treated with SCF Vivo-Morpholino (B). Data are mean ± SEM of 9 experiments for *q*PCR. *p<0.05 vs. WT SCF Mismatch; #p<0.05 vs. Mdr2$^{-/-}$ SCF Mismatch mice. Representative images x20.

Figure 6: *In vitro* evaluation of biliary SCF signaling. By immunofluorescence we found that cultured MCs express c-Kit and cultured cholangiocytes express SCF (A). Inhibition of SCF using ISCK03 (10 μM, 24 hrs) blocked the gene expression of cholangiocyte PCNA (B) and p16 and p18 (C). Data are mean ± SEM of 12-15 experiments for *q*PCR. *p<0.05 vs. cholangiocyte control. Representative images x20.

Figure 7: *In vitro* cholangiocyte SCF secretion and MC migration. By EIA we found that cholangiocyte SCF secretion decreases after inhibition using ISCK03 (10 μM, 24 hrs) (A). Boyden chambers were loaded with cholangiocytes treated either with 0.1% BSA (control) or ISCK03 (10 μM, 24 hrs) into the bottom chamber and cultured MCs were placed in the upper chamber and MC migration was measured after 24 hrs (B). MC migration was significantly blunted when cholangiocytes were treated with the SCF inhibitor, ISCK03 compared to control as shown by

Toluidine Blue staining (C). Data are mean ± SEM of 9-12 experiments for EIA and 3 experiments for migration. *p<0.05 vs. cholangiocyte control. Representative images x20.

Table 1

Antibodies (use, dilution)	Source	Catalog no.
a-SMA (IF, 1:100)	Abcam, Cambridge, UK	ab5694
CK19 (IF, 1:100)	Developmental Studies Hybridoma Bank, Univ. of Iowa, Iowa City, IA)	TROMA-III (Krt19 Antibody)
CK19 (IHC, 1:200)	Abcam, Cambridge, UK	ab52625
Desmin (IF, 1:100)	Abcam, Cambridge, UK	ab15200
Ki67 (IHC, 1:100)	Abcam, Cambridge, UK	ab15580
p16 (IF, 1:100)	Abcam, Cambridge, UK	ab189034
p18 (IF, 1:100)	Abcam, Cambridge, UK	ab192239
p21 (IF, 1:100)	Abcam, Cambridge, UK	ab188224
SCF (IF, 1:100)	Abcam, Cambridge, UK	ab64677
SYP-9 (1:250)	Abcam, Cambridge, UK	ab52636

Primers (gene name)	Source	Catalog no.
α-SMA (Acta2)	Qiagen, Valencia, CA	PPM04483A
CK19 (Krt19)	Qiagen, Valencia, CA	PPM02968A
Fibronectin (Fn1)	Qiagen, Valencia, CA	PPM03786A
p16 (Cdkn2a)	Qiagen, Valencia, CA	PPM02906F
p18 (Cdkn2c)	Qiagen, Valencia, CA	PPM02893C
p21 (Cdkn1a)	Qiagen, Valencia, CA	PPM02901B
PCNA (Pcna)	Qiagen, Valencia, CA	PPM03456A
SCF (Kitl)	Qiagen, Valencia, CA	PPM02983C
SYP-9 (Syp)	Qiagen, Valencia, CA	PPM03241A

Table 2 Characteristics of liver donors of normal controls and PSC

	Year of Birth	Sex	Pathological Diagnosis	Cirrhosis
Normal Control 1	58	Female	Normal	No
Normal Control 2	58	Female	Normal	No
Normal Control 3	62	Female	Normal	No
PSC 1	56	Female	Advanced stage	No
PSC 2	50	Female	Early - advanced stage	No
PSC 3	37	Female	Early - advanced stage	No

PSC = primary sclerosing cholangitis

Highlights:

- Mast cells migrate to the liver during damage and contribute to liver fibrosis during primary sclerosing cholangitis (PSC)
- Migration of mast cells is regulated by paracrine signals from damaged cholangiocytes
- Damaged cholangiocytes express and secrete stem cell factor (SCF) and SCF is upregulated in human PSC
- Inhibition of SCF blocks mast cell migration and ameliorates liver damage and hepatic fibrosis

The authors have no conflict of interest.

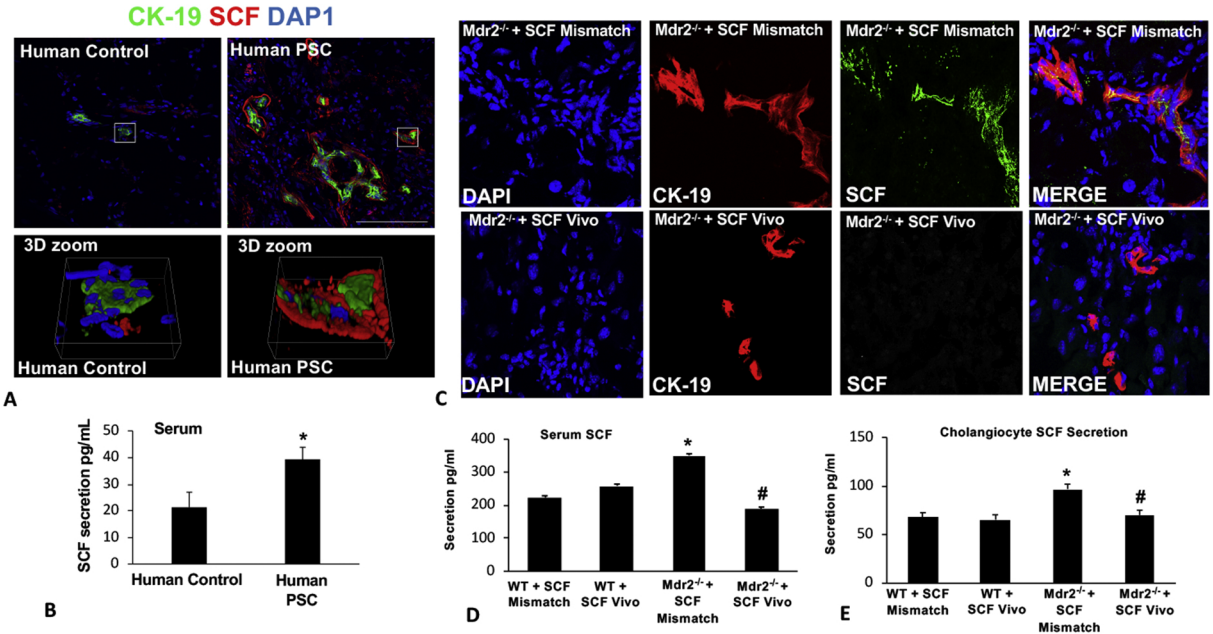
CK-19 SCF DAP1
Human Control
Human PSC
3D zoom
Human Control
3D zoom
Human PSC
A
Mdr2-/- + SCF Mismatch
DAPI
Mdr2-/- + SCF Mismatch
CK-19
Mdr2-/- + SCF Mismatch
SCF
Mdr2-/- + SCF Mismatch
MERGE
Mdr2-/- + SCF Vivo
DAPI
Mdr2-/- + SCF Vivo
CK-19
Mdr2-/- + SCF Vivo
SCF
Mdr2-/- + SCF Vivo
MERGE
C
Serum
SCF secretion pg/mL
50
40
30
20
10
0
*
Human Control
Human PSC
B
Serum SCF
Secretion pg/ml
400
300
200
100
0
*
#
WT + SCF Mismatch
WT + SCF Vivo
Mdr2-/- + SCF Mismatch
Mdr2-/- + SCF Vivo
D
Cholangiocyte SCF Secretion
Secretion pg/ml
150
100
50
0
*
#
WT + SCF Mismatch
WT + SCF Vivo
Mdr2-/- + SCF Mismatch
Mdr2-/- + SCF Vivo
E

Figure 1

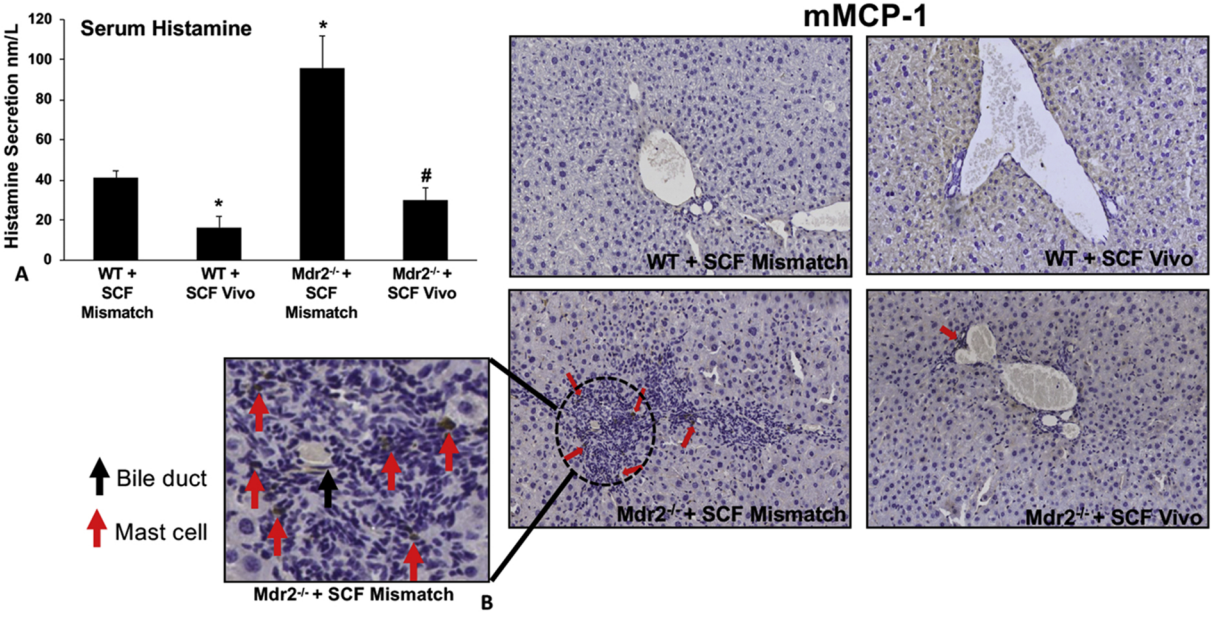
Serum Histamine
Histamine Secretion nm/L
120
100
80
60
40
20
0
*
*
#
A
WT + SCF Mismatch
WT + SCF Vivo
Mdr2-/- + SCF Mismatch
Mdr2-/- + SCF Vivo
mMCP-1
WT + SCF Mismatch
WT + SCF Vivo
Mdr2-/- + SCF Mismatch
Mdr2-/- + SCF Vivo
Bile duct
Mast cell
Mdr2-/- + SCF Mismatch
B

Figure 2

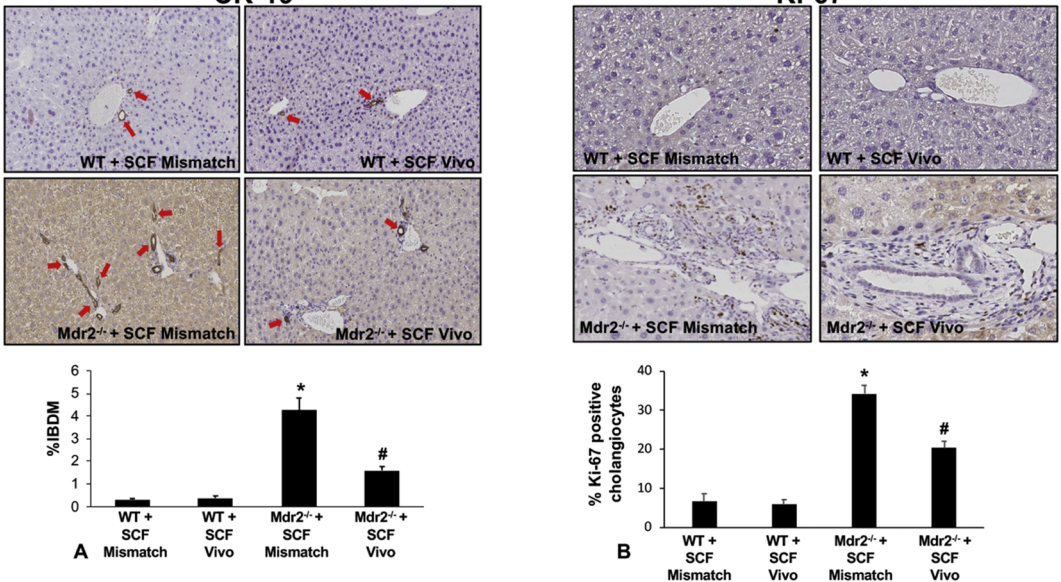
CK-19
Ki-67
WT + SCF Mismatch
WT + SCF Vivo
Mdr2-/- + SCF Mismatch
Mdr2-/- + SCF Vivo
%IBDM
% Ki-67 positive cholangiocytes
WT + SCF Mismatch
WT + SCF Vivo
Mdr2-/- + SCF Mismatch
Mdr2-/- + SCF Vivo
A
B

Figure 3

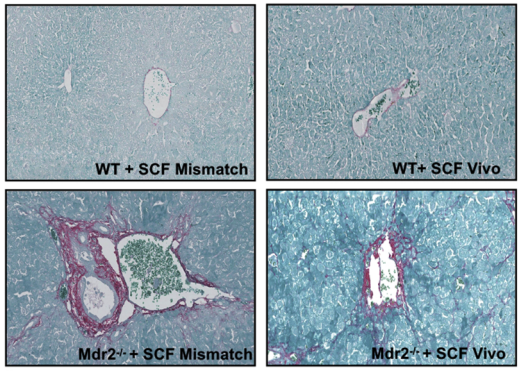
WT + SCF Mismatch
WT+ SCF Vivo
Mdr2-/- + SCF Mismatch
Mdr2-/- + SCF Vivo
A

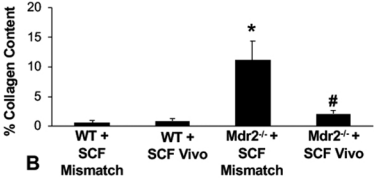
% Collagen Content
20
15
10
5
0
*
#
WT + SCF Mismatch
WT + SCF Vivo
Mdr2-/- + SCF Mismatch
Mdr2-/- + SCF Vivo
B

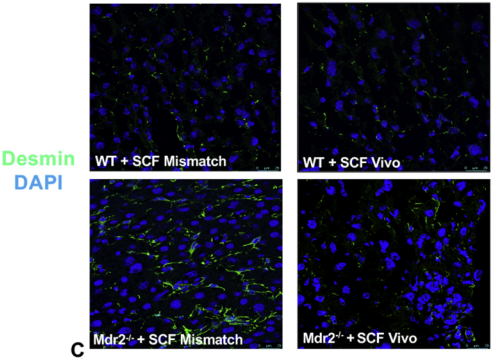
Desmin
DAPI
WT + SCF Mismatch
WT + SCF Vivo
Mdr2-/- + SCF Mismatch
Mdr2-/- + SCF Vivo
C

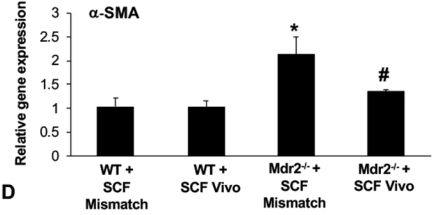
α-SMA
Relative gene expression
3
2.5
2
1.5
1
0.5
0
*
#
WT + SCF Mismatch
WT + SCF Vivo
Mdr2-/- + SCF Mismatch
Mdr2-/- + SCF Vivo
D

Figure 4

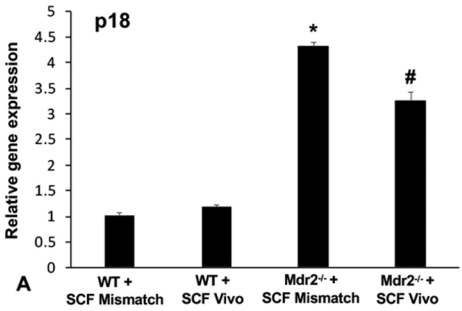
p18
Relative gene expression
5
4.5
4
3.5
3
2.5
2
1.5
1
0.5
0
*
#
A
WT + SCF Mismatch
WT + SCF Vivo
Mdr2-/- + SCF Mismatch
Mdr2-/- + SCF Vivo

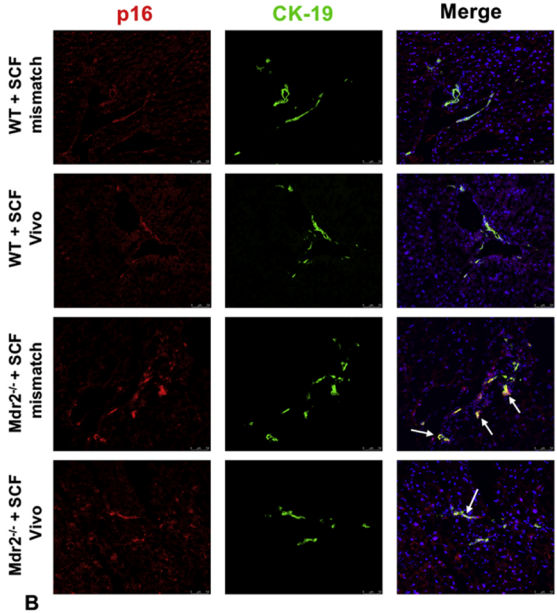
p16
CK-19
Merge
WT + SCF mismatch
WT + SCF Vivo
Mdr2-/- + SCF mismatch
Mdr2-/- + SCF Vivo
B

Figure 5

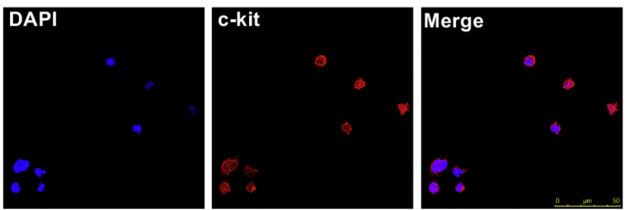

Cultured mast cells

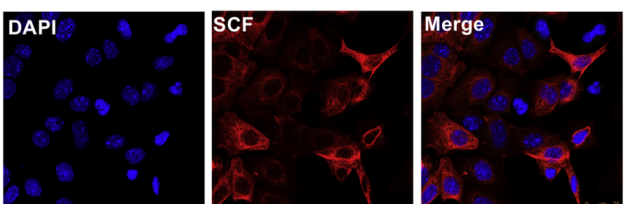

A Cultured MSE cholangiocytes

Cultured MSE cholangiocytes

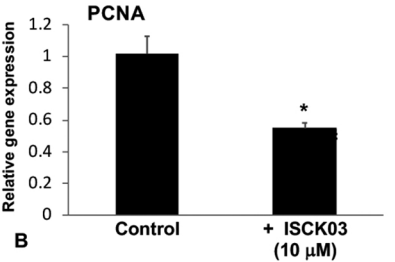

B

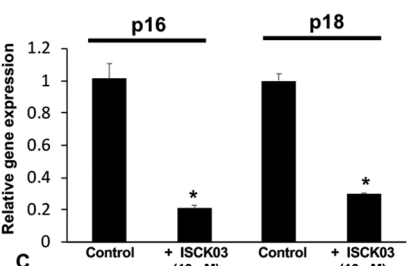

C

Figure 6

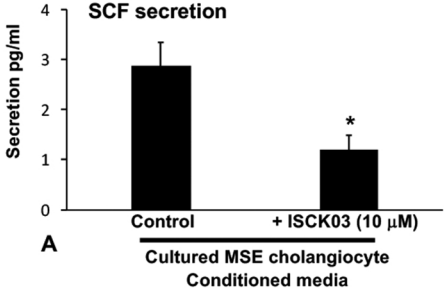
SCF secretion
Secretion pg/ml
4
3
2
1
0
*
Control
+ ISCK03 (10 μM)
A
Cultured MSE cholangiocyte
Conditioned media

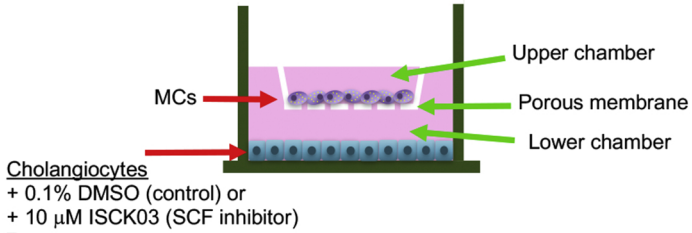
Upper chamber
MCs
Porous membrane
Lower chamber
Cholangiocytes
+ 0.1% DMSO (control) or
+ 10 μM ISCK03 (SCF inhibitor)
B

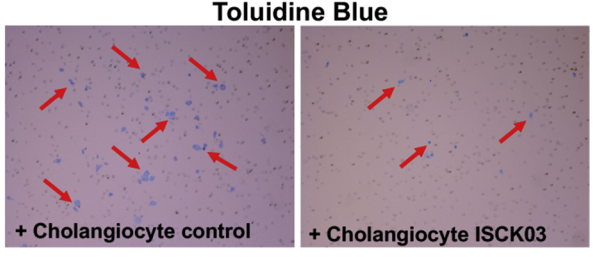
Toluidine Blue
+ Cholangiocyte control
+ Cholangiocyte ISCK03
C
Toluidine Blue positive MCs

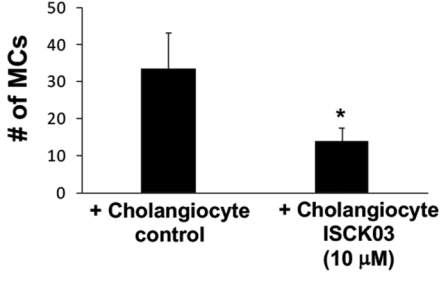
# of MCs
50
40
30
20
10
0
*
+ Cholangiocyte control
+ Cholangiocyte ISCK03 (10 μM)

Figure 7